

Comprehensive Fast Tone Mapping for High Dynamic Range Image Visualization

Jiang Duan, Guoping Qiu and Min Chen
School of Computer Science, University of Nottingham, UK
{qiu, jxd, mzc} @ cs.nott.ac.uk

Abstract: In this paper, we present a comprehensive tone reproduction curve based operator for the fast visualization of high dynamic range images. Image reproduction is a highly subjective process and different users will have very different preferences even for the same image. Therefore, a really useful tone-mapping tool for high dynamic range images should be fast and interactive, with which users can interactively adjust the mapping parameters and instantly visualize the results. Furthermore, there should be as few adjustable parameters as possible, and equally important, the parameters should have a clear, intuitive and straightforward relationship with the appearance of the mapped images to guide the users to adjust the parameters. Based on these requirements, we have developed a comprehensive tone reproduction curve based mapping technology. Our technique has two intuitive variables, which can be adjusted at an interactive speed even for very large images. One parameter controls the overall brightness of the reproduction and the other adjusts the detail and contrast¹ of the result. A piece of easy to use high dynamic range image visualization software that implements our operator is publicly available².

Key Words: Tone mapping, High dynamic range image, Visualization.

1. Introduction

Recent technologies have made it relatively easy to create radiance maps that capture the full dynamic range of real world high contrast scenes [1]. Using the method of [1], a high dynamic range (HDR) radiance map of a scene can be generated by using a sequence of low dynamic range (LDR) images of the same scene taken under different exposure intervals³. Apart from the method of [1], other techniques for capturing HDR images have also been developed by various researchers e.g., [2] and [3]. More recently, technology has also been developed to capture high dynamic range videos [7, 8].

The HDR radiance map records the full dynamic range of the scene in numerical format. However, most reproduction devices, such as computer monitors and printers, have a dynamic range of about two orders of magnitude⁴, which is significantly lower than the dynamic range of the radiance map data. In order to reproduce HDR maps in LDR

devices, mapping or tone reproduction techniques are used to map HDR values to LDR values. Tone reproduction (mapping) is a crucial step in high dynamic range digital imaging workflow, because it doesn't matter how accurate the HDR maps may be, they have to be accurately and faithfully reproduced in the LDR devices. If the reproduction techniques fail, the whole workflow fails.

In the literature, a number of techniques have been developed for tone reproduction for visualizing high dynamic range images. There are two broad categories of technology, i.e., tone reproduction curve (TRC) based and tone reproduction operator (TRO) based [10].

TRC refers to techniques that use monotonic mapping functions to transfer world luminance to display luminance. A tone reproduction method that attempted to match display brightness with real world sensations was introduced in [11]. More recently, [9] presented an adaptive logarithmic curve method for compressing high dynamic range images. Perhaps the most comprehensive technique in this category is still that of [14], which introduced a quite sophisticated tone reproduction curve technique that incorporated models of human contrast sensitivity, glare, spatial acuity and color sensitivity.

TRO techniques involve the spatial manipulation of local neighboring pixel values, often at multiple scales. The scientific principle of this type of technique is based on the image formation model: $I(x, y) = L(x, y) R(x, y)$, which states that image intensity function $I(x, y)$ is the product of the illuminant function $L(x, y)$ and the scene reflectance function $R(x, y)$. Because real world reflectance $R(x, y)$ has low dynamic range (normally not exceeding 100:1), reducing the dynamic range of $I(x, y)$ can be achieved by reducing the dynamic range of $L(x, y)$ if one could separate $L(x, y)$ from $R(x, y)$. Methods based on this principle include [15], [16] and [17]. They mainly differ in the way in which they attempted to separate the illuminant component from the reflectance component. All TRO based methods can be regarded as related to the Retinex theory [21]. A direct use of the Retinex theory for high dynamic range compression has been presented in [24].

Recent development has also attempted to incorporate traditional photographic technology in the digital domain for the reproduction of high dynamic range images [18]. An impressive technology for high dynamic range compression is that of [19]. Based on the observation that human visual system is only sensitive to relative local contrast, the authors developed a multiresolution gradient domain technique. This is also a TRO type technique and the authors reported very good results that were free from halo effects.

¹ Note that in this paper we use these terms loosely without following their strict definition.

² <http://www.cs.nott.ac.uk/~qiu/hdri/PG05/PG05.html>

³ The software for creating HDR maps is available for download from the Internet: <http://www.debevec.org/HDRShop/>

⁴ Although high dynamic range image displaying system are being developed [35], they are expensive.

TRO based methods involve multiresolution spatial processing and are therefore computationally very expensive. Because TRO methods could reverse local contrast, they sometimes can cause “halo” effects in the reproductions. Another difficulty of these techniques is that there are too many parameters the users have to set, which makes them quite difficult to use. TRC based methods do not involve spatial processing, they are therefore computationally very simple. This is useful in real time applications such as high dynamic range video [7, 8]. TRC techniques also preserve the intensity orders of the original scenes and avoid artifacts such as halo that is often associated with TRO based methods. One of the weaknesses of TRC approaches as compared with TRO methods is that it may cause noticeable lost of details in some images. Because of their respective merits and drawbacks of both technologies in terms of resulting image quality, computational complexity, simple implementation and easy to use, both types of technologies are likely to co-exist for tone mapping in HDR imaging for the foreseeable future.

In this paper, we present a comprehensive tone mapping curve based operator for fast visualization of high dynamic range images. We deliberately use the word visualization. Strictly speaking, image reproduction is device dependent, it is meaningless to talk about image reproduction without specifying a standard calibrated reproduction device since readers who are likely to use our technology will be using different uncalibrated devices. So our technology should be more accurately called a visualization technology, which allows users to quickly view HDR images. To reproduce an image means to make the image to have an appearance that faithfully reflects the original scene, this is a much more complicated and difficult task. Image reproduction is a highly subjective process and different users will have very different preferences even for the same image. Therefore, a really useful tone-mapping tool for high dynamic range images should be fast and interactive, with which users can interactively adjusting the mapping parameters and instantly visualize the results. Furthermore, there should be as few adjustable parameters as possible, and equally important, the parameters should have a clear, intuitive and straightforward relationship with the final tone-mapping results to guide the users to adjust the mapping results. Based on these requirements, we have developed a comprehensive tone reproduction curve based mapping technology. Our technique has two intuitive variables, which can be adjusted at an interactive speed even for very large images. One parameter controls the overall brightness of the reproduction and the other adjusts the details and contrast of the result. In this submission, we also provide a very easy to use software that implements of our operator.

2. A Comprehensive Adaptive Tone Mapping Curve Based Operator

In mapping high dynamic range images to low dynamic range ones for reproduction purpose, there are two basic requirements. The first is that the overall brightness should be correct and the other is that there should be enough detail in the reproduced images. Both requirements are

subjective and scene dependant. One extra difficulty faced HDR image tone reproduction operators is that the ways in which the high dynamic range radiance maps are constructed are nonstandard. The absolute luminance values of the images are not always know [1, 34], which means that we do not know how bright/dark the reproduced image should really be. It is important to point out that this fact has not always been explicitly recognized and addressed in most published HDR image tone mapping operators. In general, human observers tend to prefer images with more details, however, this is again a subjective parameter. Too much detail will make the image look artificial (many TRO-based technologies tend to do this) and not enough detail makes the image look blurry (many TRC-based technologies tend to do this). Given that this is the case we will have no choice but to rely on human judgment. Therefore, the best it can be hoped for a tone mapping operator is semiautomatic ones with the human users controlling the final results. A really useful tone mapping operator, therefore, should provide such a facility to enable users to adjust the “correct overall brightness” and the “right amount” of details in the mapped images.

In this section, we present a comprehensive tone mapping operator that provides these facilities. Our operator consists of two sub-operators. We first use an adaptive global luminance-mapping operator to compress the luminance of high dynamic range image and simultaneously set the overall brightness of the reproduction by changing a single number. The output of this first sub-operator is then adjusted to final display luminance in such a way that changing another number can easily control the “right amount” of detail and contrast in the reproduction.

2.1. Adaptive Luminance Mapping

As a first step, we use following function to compress the luminance of the high dynamic range image I to display luminance D :

$$D(I) = (D_{max} - D_{min}) * \frac{\log(I + \tau) - \log(I_{min} + \tau)}{\log(I_{max} + \tau) - \log(I_{min} + \tau)} + D_{min} \quad (1)$$

where I_{min} and I_{max} are the minimum and maximum luminance of the scene, and D_{max} and D_{min} are the minimum and maximum luminance of the visualization devices, $\tau = \alpha(I_{max} - I_{min})$, $\alpha \geq 0$. Equation (1) ensures that the maximum and minimum luminance values of the scene are respectively mapped to the maximum and minimum luminance of the visualization device. Adjusting α will appropriately tune the overall brightness of the reproduced image. Figure 1 shows plots of the mapping curve of (1) for several different α 's. It is seen that the curves distribute the world luminance to display luminance according the values of α . For example, setting $\alpha = 0$ %, the lower 20% of the world luminance will be placed at over 80% of the lower end of the display luminance. The end effect is of course, that the display will be bright. By changing the value of α , we can allocate the display luminance to world luminance differently, thus adjusting the overall brightness of the reproduction. When $\alpha \rightarrow \infty$, $D(I) = I$.

The overall brightness of the scene is also called the key of the scene in [18] which describes whether it is subjectively

light, normal or dark. A sunshine scene would have a high key value while a room with dim lighting would have a low key value. In a sense the adjustable variable τ in (1) corresponds to the key value in [18] which is used to set the overall brightness of the mapped images. Figure 2 shows an example demonstrating the effects of changing the controlling parameter τ .

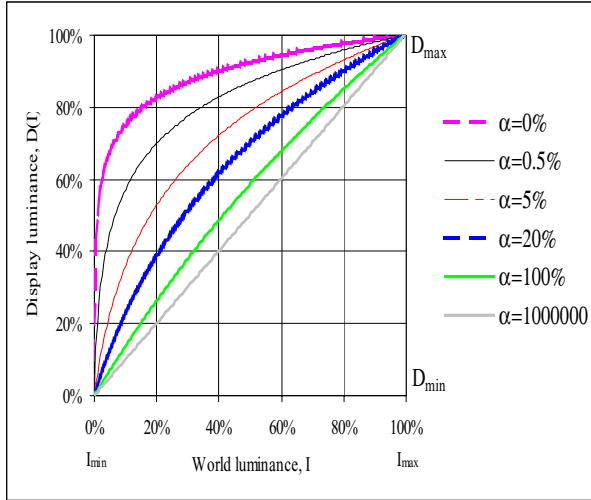


Figure 1: The global luminance-mapping curve of (1) for different values of α .

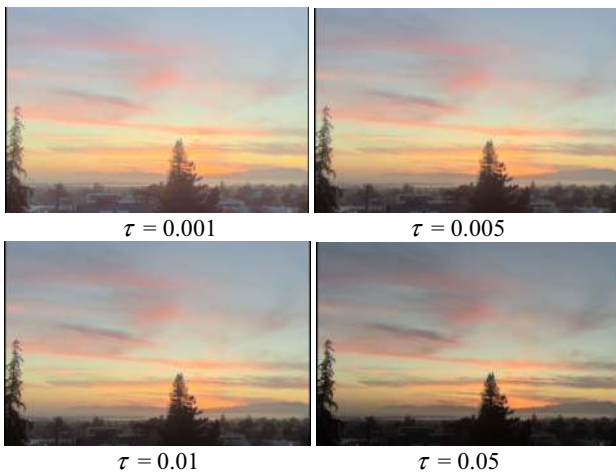


Figure 2: A high dynamic range image mapped using Equation (1) with different values of τ .

Figure 3 shows several HDR images mapped using (1) with appropriately chosen τ s. The histograms of the reproduced images are also shown in the Figure. As can be seen, although the overall brightness of the mapped image can be set appropriately, for most of the cases, the mapping function produces images that appear to not have sufficient details and appear low contrast. Inspecting the histograms of the images indicates that a typical characteristic of these histograms is that all have a narrow shape. This means that a large amount of pixels are squashed to a small portion of the available display dynamic range.

Mapping curves similar to that of Equation (1) was recommended by Stockham for image processing purpose because human visual perception is logarithmic [4]. In addition, the operation is in line with modern photography practices that favor curves that compress mainly the high

luminance values [29, 30]. For HDR image mapping, both [9] and [18] have used mapping functions of the similar shape with (1) as the initial steps of their techniques, but report similar unsatisfactory reproduction results from these simple operations. In the following session we use a fast adaptive histogram adjustment strategy to process the output of (1) mapped image before rendering it for display.

2.2. Adaptive Histogram Adjustment

After an HDR image is mapped by Equation (1), ignoring numerical errors, the output image still contains the same amount of information as the original input because the mapping function is monotonic and using $D(I)$ can completely recover the original I . The reason that rendering $D(I)$ for display will result in the lack of detail and contrast is caused by linear scaling (quantization) as illustrated in Figure 4 (a). In this case, the range of $D(I)$ is divided into equal intervals, and pixels falling into the same interval are compressed to have the same display value. Quantization is done purely on the basis of the pixel dynamic range without taking into account the image's pixel distribution characteristics. As a consequence, too many pixels are squeezed into one display value, resulting in a lost of detail and contrast, whilst in sparsely populated intervals, too few pixels occupy a valuable a display level thus resulting in the under utilization of display luminance levels.



Figure 3: Top row: some high dynamic range images mapped using Equation (1) with appropriately selected values of τ . Bottom row: the corresponding histograms of the images on the top row. Note due to the differences in reproduction devices, the “appropriate τ ” may be different for different devices. We suggest use the accompanied software to find your preferred τ .

A traditional technique that takes into account pixel distribution is histogram equalization as shown in Figure 4 (b). In this case, the method divides the range of $D(I)$ into N intervals based on the pixel distribution *only*. Within each interval, there is equal number of pixels falling onto it. The division of these intervals is purely based on the pixel population distributions and the actual pixel luminance values spanned in the intervals are not taken into account. Again pixels falling into the same interval are mapped (quantized) into the same display luminance. Although, the display luminance levels are fully utilized in such kind of circumstances, densely populated intervals can result in the exaggeration of contrast (the mapping curve is too steep), while in sparsely populated luminance intervals, compression is too aggressive (the mapping curve is too flat).

Although histogram equalization mapping makes full use of the display dynamic range, it often introduce objectionable visual artifacts (Figure 5, 6, 8). While simple linear scaling of $D(I)$ of (1) often results in the under-utilization of display dynamic range, which lead to the low contrast images (Figure 3). Fortunately the drawbacks of each of the techniques is compensated by one another. In order to achieve the desirable results, the sub-operator of our algorithm in this stage should strike a balance between the simple linear scaling and histogram equalization (Figure 4 (c)).

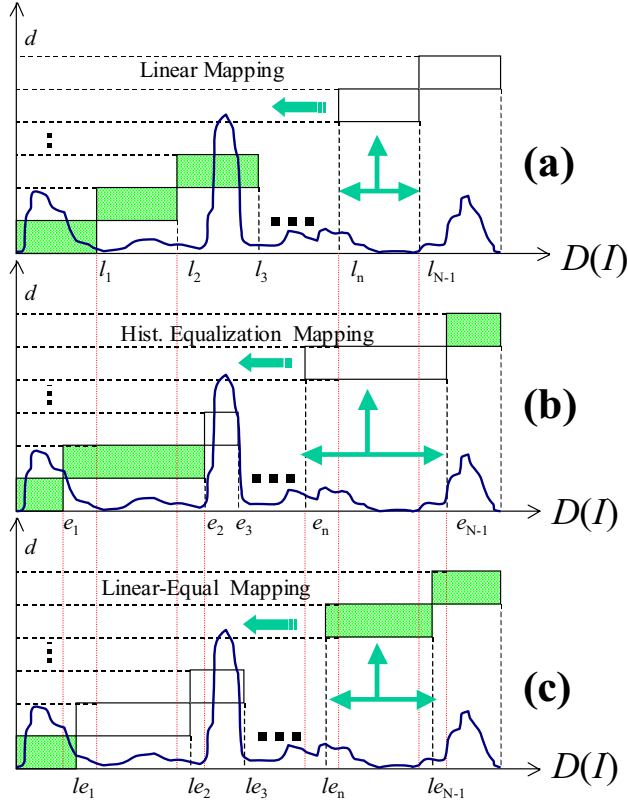


Figure 4. Mapping the output of $D(I)$ for display. (a) Linear mapping divides the luminance range into N equal length intervals and maps pixels falling into the same interval to the same display value. (b) Histogram equalization mapping divides the luminance range into N intervals such that the numbers of pixels falling into each interval are the same. All pixels falling into the same interval are again mapped to the same display value. (c) The sub-operator of our algorithm divides the luminance range into N intervals in such a way that the cuts should fall in between those of the linear scaling and histogram equalization.

Therefore, the 2nd stage of our comprehensive tone mapping operator is to take the output of the first operator $D(I)$ as input and adjust its histogram according to Figure 4 (c), i.e., to map $D(I)$ to the display image d using a curve that is between linear scaling and histogram equalization. One way to achieve this is to map the image by optimizing following objective function

$$E = \sum_{k=1}^{N-1} \left(l_{e_k} - \frac{k(D_{\max} - D_{\min})}{N} \right)^2 + \lambda \sum_{k=1}^{N-1} \left(\int_{D_{\min}}^{l_{e_k}} h(x) dx - \frac{k}{N} \int_{D_{\min}}^{D_{\max}} h(x) dx \right)^2 \quad (2)$$

where $h(x)$ is the histogram and λ is the Lagrange multiplier. Setting $\lambda = \infty$, optimizing E becomes histogram

equalization mapping, and $\lambda = 0$, optimizing E becomes linear scaling mapping. By choosing an appropriate λ , we can strike a balance between the two extreme forms of mapping to suit individual images. An optimal solution to (1) can be found by solving following linear equations.

$$\frac{\partial E}{\partial l_{e_k}} = 0 \quad k = 1, 2, \dots, N-1 \quad (3)$$

However, Equation (3) is seriously under constrained, and a straightforward numerical solution to optimize E in (2) may be difficult to obtain.

Here we use a more intuitive approach [33] to perform the mapping of Figure 4(c). With reference to Figure 4, for linear mapping, the luminance axis is cut at l_1, l_2, \dots, l_{N-1} . For histogram equalization, the luminance axis is cut at e_1, e_2, \dots, e_{N-1} . Our operator cut the luminance axis at $l_{e_1}, l_{e_2}, \dots, l_{e_{N-1}}$, which satisfy following relation

$$l_{e_n} = l_n + \beta(e_n - l_n) \quad (4)$$

where $0 \leq \beta \leq 1$ is a controlling parameter. If $\beta = 0$, the mapping is linear, $\beta = 1$, the mapping is histogram equalized. Setting $0 < \beta < 1$, we control the mapping between linear scaling and histogram equalized in a simple and elegant manner.

In practice, the sub-operator recursively bi-partitions the $D(I)$ axis. It first finds the cut that divides the $D(I)$ into two equal length intervals (linear mapping to two levels), then another cut such that the numbers of pixel on either side of the cut is identical and equal to half of the total pixel population (histogram equalization mapping to two levels). It then finds a cut that is between these two cuts using Equation (4). In this way the pixels are divided into two groups. Each group is then subsequently and independently divided into two groups following the same procedure. After n iterations, the dynamic range would have been divided into $N = 2^n$ segments. Pixels that fall into the same segments are then mapped to the same display luminance in the low dynamic range devices.

The only control parameter the user has to set in this stage of the algorithm is β . If $\beta = 0$, the adjustment is linear, if $\beta = 1$, the adjustment is histogram equalized. Setting $0 \leq \beta \leq 1$, we control the mapping between linear and histogram equalized in a very simple and elegant way. In contrast to many other methods where the setting of parameter values is *ac hoc*, setting β has a clear meaning and directly relates to the appearances of the mapped image. For most images, setting $\beta = 0$ will result in lack of details and contrast whilst setting $\beta = 1$ will result in visually annoying artifacts. By setting a single parameter $0 \leq \beta \leq 1$ we can strike a balance. In fact our experiences showed that by setting $\beta = 0.5$ as default worked very well for a variety of images. Again, we refer readers to the accompanied software to test out the effects of β .

The adaptive histogram adjustment operation assigns relatively more display values to the densely populated intervals and relatively fewer display values to the sparsely populated intervals in the range of $D(I)$, which is a reasonable strategy in terms of efficient encoding. For such an operation, in the densely populated intervals the

mapping curve will be relatively steep (but will be smoother than that of histogram equalization), in the sparsely populated intervals, the mapping curve will be relative smooth (but will be steeper than that of histogram equalization), as illustrated in Figure 5.

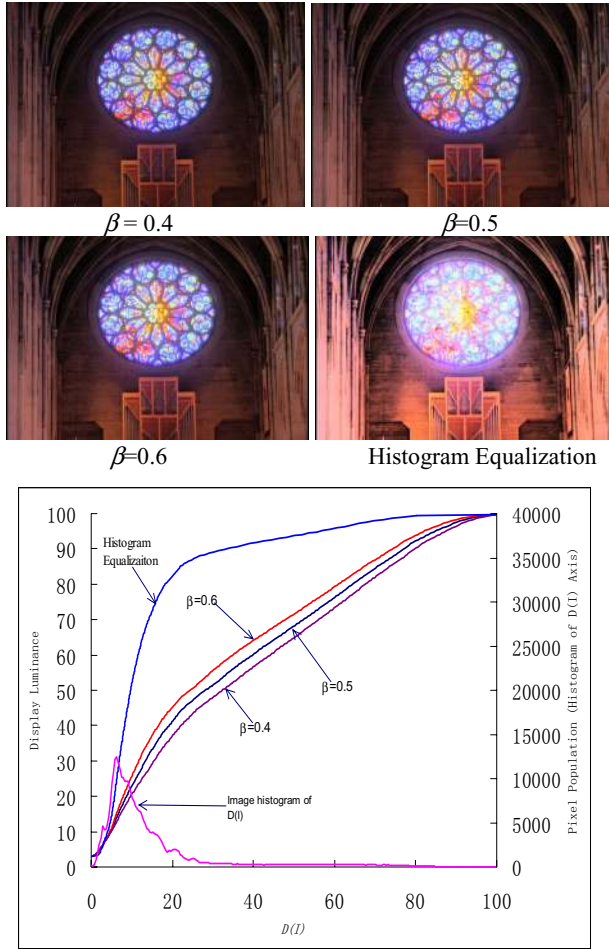


Figure 5. Top two rows: Rosette images mapped by our comprehensive tone reproduction operator with $\tau = 0.1$ and various β values and histogram equalization. Bottom row: The Rosette image's Adaptive Histogram Adjustment transferring curves of our operators and histogram equalization transferring curve in the space of Display Luminance against $D(I)$.

3. Experimental Results

The technique has been tested on a wide variety of high dynamic range images. In our experiments, the luminance signal is calculated as: $L = 0.299R + 0.587G + 0.114B$. Similar to other HDR image tone mapping operators, we only map the luminance channel into display luminance. This is achieved in two steps. First, the HDR luminance is mapped by Equation (1). Second, the output of the first step is used to construct a high resolution histogram (in the order of 100,000 bins), and the adaptive histogram adjustment technique of section 2.2 is then used to adjust $D(I)$ to display luminance. After mapping, the LDR images are rendered for display using following formula

$$R_{out} = \left(\frac{R_{in}}{L_{in}}\right)^\gamma L_{out}, G_{out} = \left(\frac{G_{in}}{L_{in}}\right)^\gamma L_{out}, B_{out} = \left(\frac{B_{in}}{L_{in}}\right)^\gamma L_{out} \quad (5)$$

where L_{in} and L_{out} are luminance values before and after compression, γ controls display color (setting it between 0.4 and 0.6 worked well).

The methods are computationally very simple. On a standard Pentium 4 PC, the parameters can be adjusted at an interactive speed even for images as large as 1024x769 pixels, making the effects of parameter changing instantly visible. The two parameters, α controls the overall brightness of the display and β controls the amount of details and contrast of the display. In this section, we present results of our comprehensive tone reproduction operator. The software is also available at <http://www.cs.nott.ac.uk/~giu/hdri/PG05/PG05.html> (submitted to PG'05 as extra materials).

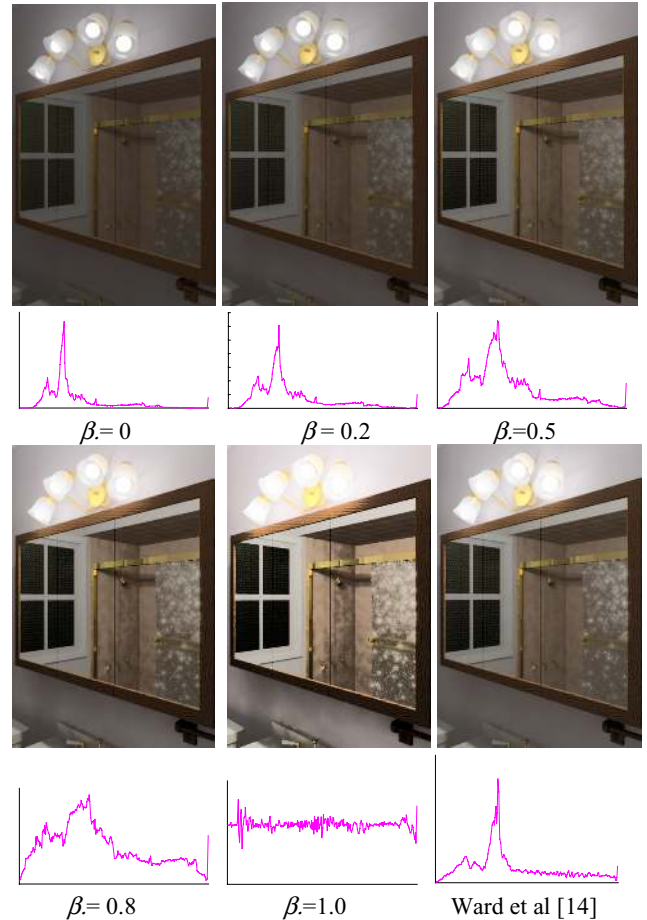


Figure 6. The Bathroom image mapped by our comprehensive tone reproduction operator with $\tau = 0$ and various β values. In the monitor we used, setting $\tau = 0$ gives a display with appropriate overall brightness. For different reproduction device, this value may have to be set differently, please try this out using the accompanied software. It is seen that as β increases, the mapping approaches histogram equalization and for this image setting $\beta = 0.5$ seems to be the best.

Figure 6 shows the result of the Bathroom image mapped by our tone mapping operator for $\tau = 0$ and various β values and these of Ward et al [14] and histogram equalization ($\beta=1.0$). Figure 7 shows these overall mapping curve of these operators for the bathroom image. It is seen that for this image, there are very few very bright pixels

(corresponding to the area of the lamps), yet these are very important pixels. Histogram equalization clearly compresses these pixels too aggressively, so does the method of Ward et al [14] because this is essentially an approximate histogram equalization method in treating sparsely populated intervals. This fact is demonstrated clearly in Figure 7 where a very short display luminance interval has been allocated to the very bright part of the world luminance by both the histogram equalization and Ward et al's method [14]. In contrast, our method is more flexible and by adjusting β , we can flexibly assigned more display intervals to the very bright world luminance interval and retain more details in this area.

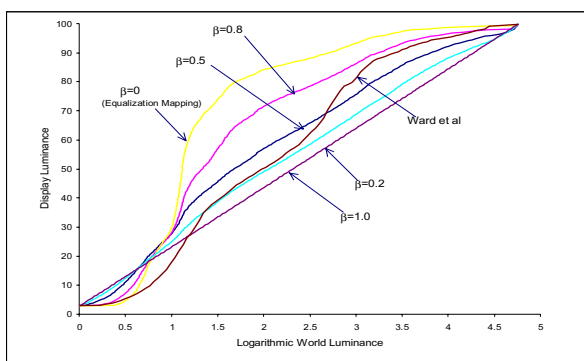


Figure 7. The Bathroom image's mapping curves of various operators.

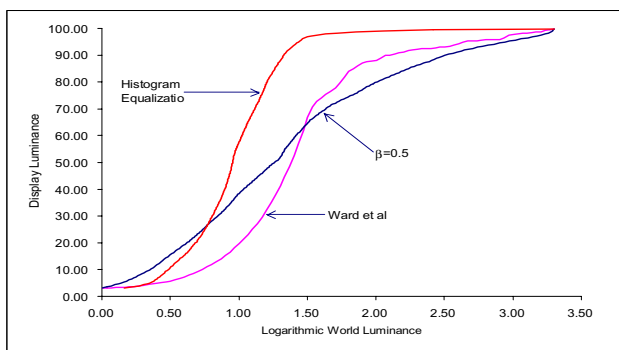
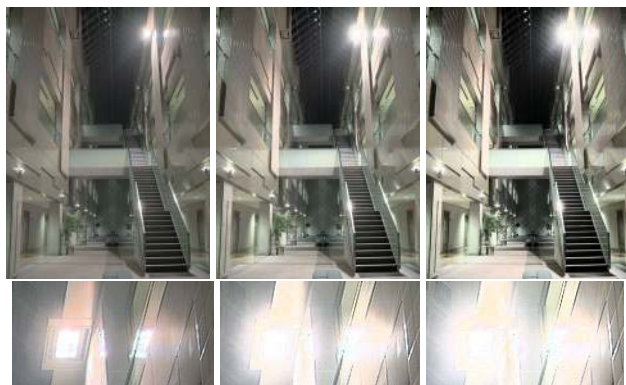


Figure 8. Top row: left to right, AtriumNight images mapped by our new method for $\tau = 0.5$ and $\beta = 0.5$, the method of Ward et al [14] and histogram equalization. Middle row: amplified regions of the images above them. In our monitor, setting $\tau = 0.5$ seems to give the most appropriate overall brightness for this image. Bottom row: Tone mapping curves for the image.

Figure 8 shows another example of the mapping results and mapping curves of our operators and those of histogram equalization and Ward et al's [14]. Again, for this image, there are very few very bright pixels, Ward et al's method and histogram equalization again have compressed these bright parts too aggressively as demonstrated clearly in the mapped images and the mapping curves of various methods. It is shown clearly the areas of the lamps in the images mapped by Ward et al's method and histogram equalization have been saturated because compression is too aggressive in this part and not enough display levels have been allocated to this part, this fact is demonstrated more clearly in the mapping curves. In contrast our algorithm keeps more details in the part of the image.

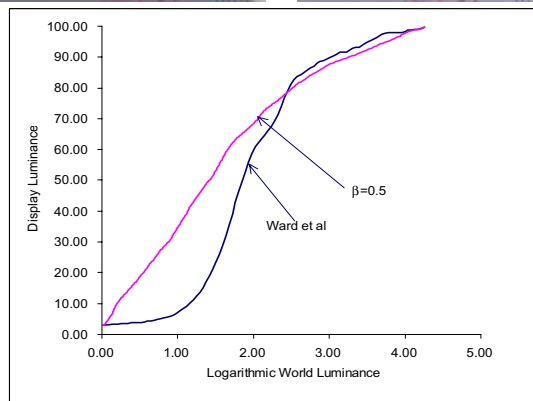
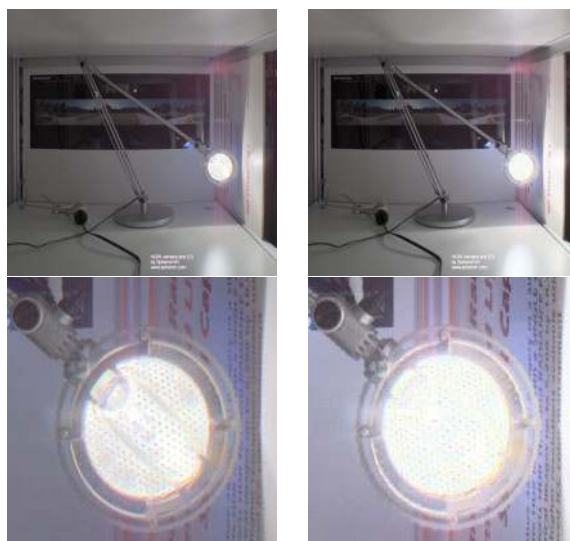


Figure 9. Top row: left to right, images mapped by our new method for $\tau = 0$ and $\beta = 0.5$ and the method of Ward et al [14]. Middle row: amplified regions of the images above them. Again, in our monitor, setting $\tau = 0$ seem to give the most appropriate overall brightness. Bottom row: Tone mapping curves for the lamp image.

Figure 9 shows yet another example of the mapping results of our operator and that of Ward et al's. Again, in this image, the very bright area (the lamp) is very small compared to the image size. Compared with Ward et al [14], our operator was able to allocate more display values to this very bright part of the image. As a result, in our image, detail of the lamp is visible whilst in the image

mapped by the method of [14] the lamp has become saturated and very little detail is visible.

Our operator is related to the histogram adjustment technique of [14] in the sense that both manipulate the histogram. In fact, we were encouraged by the results of [14] in which the authors demonstrated that simple histogram manipulation may offer an optimal solution if the goals are to produce “good, natural looking image without regard to how well a human observer would be able to see in the real environment”. However, the histogram adjustment method of [14] has several drawbacks. Firstly, The method only caps the display contrast (mapped by histogram equalization) when it exceeds that produced by a linear tone mapping operator and the idea is further refined by human contrast sensitivity. However, in sparsely populated luminance intervals, compression is approximately achieved by histogram equalization. This means that some sparse areas that span a wide range will be compressed too aggressively. Features (details) in such intervals which are visible to human eyes could be lost. This unsatisfactory aspect of this algorithm is clearly illustrated in the examples in Figures 6 – 9. Secondly, if the dynamic range of the scene is already in the device range, the method of [14] uses linear scaling. However, as it is well known that sometimes linear mapping would result in the under utilization of display levels and thus leading to low contrast images, even though the dynamic ranges of the scenes fit within that of the visualization devices. Our method overcomes these drawbacks and offers a more comprehensive histogram adjustment solution to the mapping of HDR images. These results have clearly demonstrated the better performance of our method.

From Figure 6 to Figure 9, it is seen that at the very bright part of the images, our mapping has less aggressive compression. This is reflected in the mapped images. It is seen that in areas surrounding the lamps, our mapping has retained more details than the method of [14] and histogram equalization. This can be explained by inspecting the mapping curves, where it is seen that our mapping curve has reserved more display levels for the bright part of the intensity intervals. The reason that the method of [14] compresses the dynamic range in this interval so aggressively is because, the method is based on approximate histogram equalization (by accumulating pixel population) to produce its mapping curve, however, pixel population in this interval is sparse, the display produced in this region by the mapping curve will have low contrast and in such case the algorithm of [14] does nothing but follows histogram equalization mapping. What a good mapping should do is to be able to adjust the number of display levels assigned to such sparsely populated intervals and it is seen that our method can do just that.

As an informal comparison of results, Figure 10 shows the Memorial Church image mapped by various methods in the literature. Figure 11 show more examples of results mapped by our new operator.

4. Conclusions

In this paper, we have presented a computationally efficient and very simple and easy to use high dynamic range image tone mapping techniques. Our techniques are tone reproduction curve based hence are computationally much more efficient than many other techniques that require spatial processing. Our methods are very simple to use. Two single parameters (in fact one parameter because β can be fixed to 0.5), which have straightforward relationship with the mapped images, control the appearances of the mapped images in a simple and elegant manner. Experimental results have further demonstrated that the new methods can produce good results on a wide variety of high dynamic range images. Our methods’ performances compare favorably with state of the art while at the same time having the advantages of being computationally simple and practically easy to use. We believe our method is a useful tool for the visualization of high dynamic range image.

Acknowledgments

We thank Greg Ward for making his Radiance software available for creating the results of his technique, without which our comparison would have been impossible. We also thank Paul Debevec and all the authors who make the HDR data publicly available.

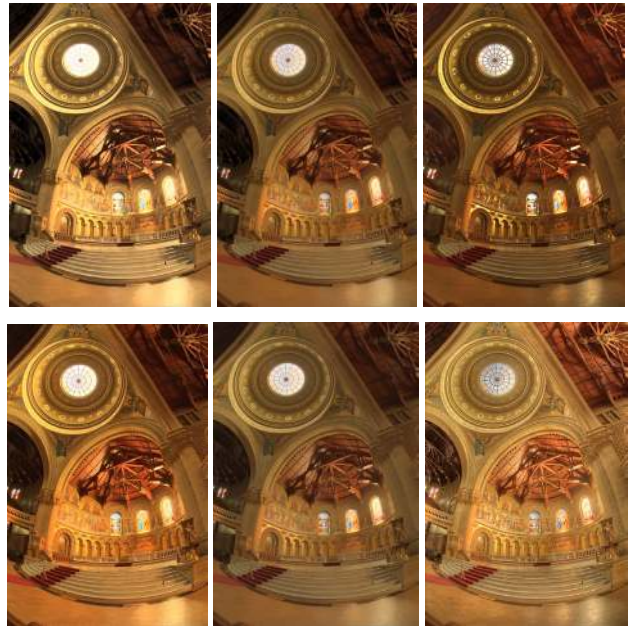


Figure 10, Tone mapping results of the Memorial Church image. From top to bottom and left to right: Result of Ward Larson [14]. Result of our new operator, $\tau=0$ and $\beta = 0.5$. Result of Bilateral filtering [17]. Result of photographic tone reproduction [18]. Result of adaptive logarithmic mapping [9]. Result of the gradient domain method [19]. All images are courtesy of various authors and printed with permission.

References

1. P. E. Debevec and J. Malik, "Recovering high dynamic range radiance maps from photographs", Proc. ACM SIGGRAPH'97, pp. 369 – 378, 1997
2. T. Mitsunaga and S. K. Nayar, "High dynamic range imaging: Spatially varying pixel exposures", Proc. CVPR'2000, vol. 1, pp. 472-479, 2000
3. S. Mann and R. W. Picard, "On being 'undigital' with digital cameras: extending dynamic range by combining differently exposed pictures", IS&T's 48th Annual Conference, Society for Imaging Science and Yechnology, Washington D. C., pp. 422 – 428, 1995
4. T.G. Stockham. Image Processing in the Context of a Visual Model, Proceedings of the IEEE, 60:828–842
5. J. Blinn. Dirty Pixels. IEEE Computer Graphics & Applications, 9(4):100–105, 1989.
6. G. Ward. Real Pixels. Graphics Gems II. Academic Press, 80–83, 1991.
7. S. B. Kang, M. Uyttendale, S. Winder and R. Szeliski, "High dynamic range video", ACM Transactions on Graphics, vol.22, no. 3, Pages: 319 – 325, July 2003
8. R. Mantiuk, G. Krawczyk, K. Myszkowski, and H-P Seidel, "Perception-motivated High Dynamic Range Video Encoding", Proc. of SIGGRAPH'2004, pp. 733-741, 2004
9. F. Drago, K. Myszkowski, T. Annen and N. Chiba, "Adaptive Logarithmic Mapping For Displaying High Contrast Scenes", The Journal of Computer Graphics Forum, Vol.22, No. 3, pp. 419-426, 2003.9
10. J. DiCarlo and B. Wandell, "Rendering high dynamic range images", Proc. SPIE, vol.3965, pp. 392 – 401, 2001
11. J. Tumblin and H. Rushmeier, "Tone reproduction for realistic images", IEEE Computer Graphics and Applications, vol. 13, pp. 42 – 48, 1993
12. M. Ashikhmin, "A tone mapping algorithm for high contrast images", Proc. Eurographics Workshop on Rendering, pp. 145 – 156, 2002
13. Greg Ward. "A contrast-based scalefactor for luminance display". In Graphics Gems IV, pages 415–421. Academic Press, 1994.
14. G. W. Larson, H. Rushmeier and C. Piatko, "A visibility matching tone reproduction operator for high dynamic range scenes", IEEE Trans on Visualization and Computer Graphics, vol. 3, pp. 291 – 306, 1997
15. K. Chiu, M. Herf, P. Shirley, S. Swamy, C. Wang and K. Zimmerman, "Spatially nonuniform scaling functions for high contrast images", Proc. graphics Interface'93, pp. 245 – 253, 1993
16. J. Tumblin and G. Turk, "LCIS: A boundary hierarchy for detail preserving contrast reduction", In Proc. of ACM SIGGRAPH'99, pp. 83-90.
17. F. Durand and J. Dorsey, Fast bilateral filtering for the display of high-dynamic-range images. ACM Trans. Graph. (special issue SIGGRAPH 2002) 21, 3, 257-266, 2002
18. E. Reinhard, M. Stark, P. Shirley and J. Ferwerda, "Photographic tone reproduction for digital images". ACM Trans. Graph. (special issue SIGGRAPH 2002) 21, 3, 267-276, 2002.
19. R. Fattal, D. Lischinski and M. Werman, "Gradient domain high dynamic range compression". ACM Trans. Graph. (special issue SIGGRAPH 2002) 21, 3, 249-256, 2002
20. Erik Reinhard, 'Parameter Estimation for Photographic Tone Reproduction', Journal of Graphics Tools, Volume 7, Issue 1, pp 45-52, 2002.
21. E. H. Land and J. J. McCann, "Lightness and retinex theory", Journal of the Optical society of America, vol. 61, pp. 1-11, 1971
22. S. N. Pattanaik, James A. Ferwerda, Mark D. Fairchild, and Donald P. Greenberg, "A Multiscale Model of Adaptation and Spatial Vision for Realistic Image Display", Proceedings of SIGGRAPH'98, pp. 287-298, Orlando, July 1998
23. J. A. Ferwerda, S. N. Pattanaik, P. Shirley and D. P. Greenberg. " A model of visual adaptation for realistic image synthesis ". Proceedings of SIGGRAPH'96, pp. 249-258.
24. D. J. Jobson, Z. Rahman and G. A. Woodell, "A multiscale Retinex for bridging the gap between color images and the human observation of scenes", IEEE Transactions on Image processing, vol. 6, pp. 965-976, 1997
25. J. Duan, G. Qiu and G. D. Finlayson, "Learning to display high dynamic range images", CGIV'2004, IS&T's Second European Conference on Color in Graphics, Volume 2, pp. 542-547 2004
26. Ferschin, P. Tastl, I. Purgathofer, W. "A comparison of techniques for the transformation of radiosity values to monitor colors", Proc. IEEE Conference on Image Processing, Austin Texas, 1994
27. R. M. Gray and D. L. Neuhoff, "Quantization", IEEE Transactions on Information Theory, vol. 44, no. 6, pp. 2325 – 2383, 1998
28. D. Marr, Vision, W. H. Freeman and Co., 1982
29. E. N. Mitchell, Photographic Science. John Wiley and Sons, New York., 1984
30. L. Stroebel, J. Compton, I. Current and R. Zakia, Basic photographic materials and processes, second ed. Focal Press, 2000.
31. R. Hall, Illumination and color in computer generated imagery, Spinger-Verlag, 1989
32. G. Qiu and J. Duan, "An Optimal Tone Reproduction Curve Operator for the Display High Dynamic Range Images", Proc. IEEE ISCAS'2005, Kobe, Japan, May 2005
33. J. Duan and G. Qiu, "Fast Tone Mapping for High Dynamic Range Images", ICPR2004, 17th International Conference on Pattern Recognition, Volume 2, pp. 847-850, 2004
34. Pattanaik Sumanta, & Yee Hector. 2002. Adaptive gain control for high dynamic range image display. Proceedings of the 18th spring conference on Computer graphics, pp. 83-87 2002.
35. Helge Seetzen, Wolfgang Heidrich, Wolfgang Stuerzlinger, Greg Ward, Lorne Whitehead, Matthew Trentacoste, Abhijeet Ghosh, Andrejs Vorozcovs, "High Dynamic Range Display Systems", ACM Transactions on Graphics (Siggraph 2004), 23(3): 760-768.



$\tau=0.1, \beta=0.5$



$\tau=0.01, \beta=0.5$



$\tau=0.0, \beta=0.5$



$\tau=0.0, \beta=0.5$



$\tau=0.001, \beta=0.5$



$\tau=0, \beta=0.5$

Figure 11. More examples of our mapping results. Please note that these parameters were visually judged to be appropriate on our monitor. Different monitors may need to adjust the parameters accordingly.